

Preparation and Characterization of $\text{H}_4\text{SiMo}_{12}\text{O}_{40}$ /Poly(vinyl alcohol) Fiber Mats Produced by an Electrospinning Method

Jian Gong,^{1,3} Xiang-Dan Li,² Bin Ding,² Douk-Rae Lee,³ Hak-Yong Kim³

¹Department of Chemistry, Northeast Normal University, Changchun 130024, People's Republic of China

²Department of Advanced Organic Materials Engineering, Chonbuk National University, Chon-ju 561-756, South Korea

³Department of Textile Engineering, Chonbuk National University, Chon-ju 561-756, South Korea

Received 19 September 2002; accepted 7 November 2002

ABSTRACT: For the first time, high-percentage molybdosilicic acid fiber mats (20–80% $\text{H}_4\text{SiMo}_{12}\text{O}_{40}$) were prepared using the electrospinning technique. The fiber mats were characterized by IR, XRD, and DSC. The results indicated that poly(vinyl alcohol) was changed from a semicrystalline to an amorphous state with an increasing molybdosilicic acid content. The results from scanning electron microscopy (SEM) showed that the average diameter of the fibers was about 285–600 nm. The effects of the viscosity and conduc-

tivity of the $\text{H}_4\text{SiMo}_{12}\text{O}_{40}$ /poly(vinyl alcohol) solution on the morphologies of the fiber mats were investigated. The swelling properties of the fiber mats in water were also studied. © 2003 Wiley Periodicals, Inc. *J Appl Polym Sci* 89: 1573–1578, 2003

Key words: differential scanning calorimetry (DSC); fibers; scanning electron microscopy (SEM); swelling; X-ray

INTRODUCTION

Hybrid inorganic–organic materials have received increasing attention over the last few years as a result of their specific properties.¹ These new materials have the possibility of becoming very useful, having both the advantages of organic materials such as light weight, flexibility, and good moldability and of inorganic materials such as high strength, heat stability, and chemical resistance.²

The electrospinning technique has been known since the 1930s.³ This technique involves a simple, rapid, inexpensive, electrostatic, nonmechanical method and has been recently rediscovered for applications such as in high-performance filters,⁴ biomedicine,⁵ and fiber templates for the preparation of functional nanotubes.⁶ These thin fibers of hybrid inorganic–organic materials have many novel properties and applications, such as opacity because of the refractive index difference between the fiber and the matrix.⁷ Another excellent application is thin fiber for scaffolds in tissue engineering⁸ that utilize the unique characteristics of the high surface area provided by the fibers.⁹ Obviously, it is important to make specific ma-

terials combined with the advantages of inorganic–organic hybrids and thin fibers together.

Polyoxometalate is an inorganic metal oxygen cluster anion, from a class of inorganic compounds that shows an unmatched applied perspective in terms of synthetic chemistry, analytical chemistry, biology, medicine, and materials science.¹⁰ Although the first polyoxometalate was reported over 170 years ago,¹¹ polyoxometalate as an inorganic–organic hybrid material has received considerable attention only recently.^{12,13} It has been found to be an extremely versatile inorganic building block for the construction of functional solid materials.¹⁴ So, to design and synthesize a polyoxometalate-based nanocomposite is significant in exploring the novel functional properties and morphology of this type of hybrid.

In the present work, we report $\text{H}_4\text{SiMo}_{12}\text{O}_{40}$ fiber mats prepared with a poly(vinyl alcohol) (PVA) additive using the electrospinning technique. The fiber mats were characterized by infrared (IR), X-ray diffraction (XRD), and differential scanning calorimetry (DSC). The swelling properties of the fiber mats were investigated.

EXPERIMENTAL

Materials and equipment

All the chemicals used were of analytical grade. FTIR studies were carried out on an Impact 410 FTIR spectrophotometer in the range of 400–4000 cm^{-1} on the

Correspondence to: H.-Y. Kim (khy@moak.chonbuk.ac.kr).

Contract grant sponsor: Chonbuk National University, South Korea.

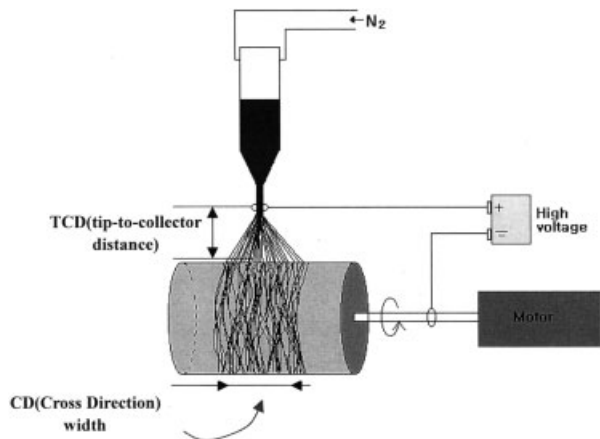


Figure 1 Schematic of the electrospinning process.

fiber mats. The DSC thermal properties of the fibers were determined with a DuPont Model 2100 DSC instrument in a nitrogen atmosphere. The scan was carried out at a heating rate of 10°C/min from 50 to 250°C. For the scanning electron microscope (SEM) investigation, an Amray 3000 SEM was used. X-ray patterns were recorded using a Philips diffractometer with a Geiger counter connected to a computer. Scans were made from 1° to 30° (2θ) at a rate of 3°/min; Ni-filtered $\text{CuK}\alpha$ radiation was used. The viscosity of the $\text{H}_4\text{SiMo}_{12}\text{O}_{40}$ /PVA solution was measured by a Brookfield Programmable DV-III+ rheometer. The conductivity of the solution was obtained with a CM-40G EC meter. For testing of the degree of swelling of each sample, the gravimetric method was used. The test pieces were immersed in water for a given time, wiped thoroughly, and reweighed. It was found that the equilibrium degree of swelling was attained after an immersion time of 24 h. The degree of swelling was calculated according to the relation $Q = (m - m_0)/m_0$, where m_0 is the weight of the unswelled sample, and m , its weight after swelling in water.

Sample preparation

$\text{H}_4\text{SiMo}_{12}\text{O}_{40}$ was supplied by the Fluka Co., Inc. (Japan). PVA had an M_n of 86,000 (96% hydrolyzed) and was supplied by the DC Chemical Co., Ltd. (South Korea).

Twenty grams of an aqueous PVA solution of 10 wt % was added to a certain amount of $\text{H}_4\text{SiMo}_{12}\text{O}_{40}$ (0.5, 2, and 8 g, respectively) with stirring for 24 h at ambient temperature. The electrospinning apparatus is shown in Figure 1. The $\text{H}_4\text{SiMo}_{12}\text{O}_{40}$ /PVA solution was contained in a plastic capillary tube. The capillary tube was then clamped to a ring stand that was above a grounded tubular layer. The tubular layer was covered by a piece of aluminum foil. A copper pin connected to a high-voltage generator was placed in the solution, and the solution was kept in the capillary by

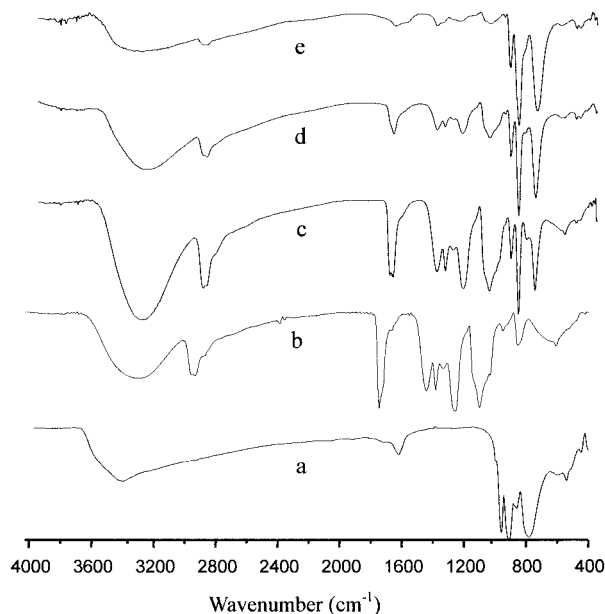


Figure 2 FTIR spectra of various $\text{H}_4\text{SiMo}_{12}\text{O}_{40}$ /PVA fiber mats with different $\text{H}_4\text{SiMo}_{12}\text{O}_{40}$ content: (a) SiMo_{12} ; (b) PVA; (c) 20 wt %; (d) 50 wt %; (e) 80 wt %.

adjusting the angle between the capillary and the aluminum foil. The distance from tip to collector was 10 cm. A voltage of 18 kV was applied to the solution and a dense web of fibers was collected on the aluminum foil. These $\text{H}_4\text{SiMo}_{12}\text{O}_{40}$ /PVA fiber mats were dried under a vacuum for 12 h at 70°C.

RESULTS AND DISCUSSION

IR spectra

Figure 2 shows IR of the fiber mats with different compositions. The O—H stretching vibration at about

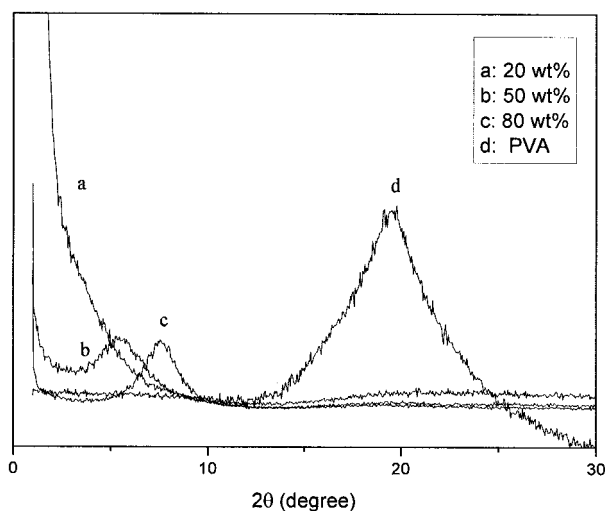


Figure 3 XRD of various $\text{H}_4\text{SiMo}_{12}\text{O}_{40}$ /PVA fiber mats with different $\text{H}_4\text{SiMo}_{12}\text{O}_{40}$ content.

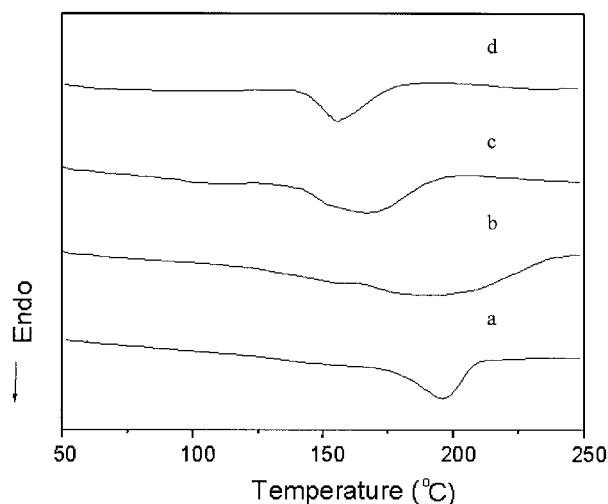


Figure 4 DSC thermogram of various $\text{H}_4\text{SiMo}_{12}\text{O}_{40}$ /PVA fiber mats with different $\text{H}_4\text{SiMo}_{12}\text{O}_{40}$ content: (a) PVA; (b) 20 wt %; (c) 50 wt %; (d) 80 wt %.

3350 cm^{-1} became a broader band with an increasing $\text{H}_4\text{SiMo}_{12}\text{O}_{40}$ content. This indicated the presence of intermolecular bonding.¹⁵ $\text{H}_4\text{SiMo}_{12}\text{O}_{40}$ with a Keggin structure consisted of one SiO_4 tetrahedron surrounded by four Mo_3O_{13} sets formed by three-edge-sharing octahedra. There were four kinds of oxygen atoms in the $\text{H}_4\text{SiMo}_{12}\text{O}_{40}$, that is, O_a (oxygen in SiO_4 tetrahedron), O_b (corner-sharing oxygen between different Mo_3O_{13} sets), O_c (edge-sharing oxygen bridge within Mo_3O_{13} sets), and O_d (terminal oxygen atom). There were four characteristic bands: 988 cm^{-1} , $\nu_{\text{as}}(\text{Mo}-\text{O}_d)$; 890 cm^{-1} , $\nu_{\text{as}}(\text{Mo}-\text{O}_b-\text{Mo})$; 796 cm^{-1} , $\nu_{\text{as}}(\text{Si}-\text{O}_a)$; and 767 cm^{-1} , $\nu_{\text{as}}(\text{Mo}-\text{O}_c-\text{Mo})$, in the IR spectra.¹⁶ Compared with the intensity of the characteristic bands of $\text{H}_4\text{SiMo}_{12}\text{O}_{40}$, the intensity of the carbonyl($\text{C}=\text{O}$) stretching band at 1733 cm^{-1} for PVA

decreased with an increasing $\text{H}_4\text{SiMo}_{12}\text{O}_{40}$ content. As a result of intermolecular H-bonding between H_3O^+ of $\text{H}_4\text{SiMo}_{12}\text{O}_{40}$ and the residual carbonyl moieties of the support polymer PVA were formed.¹⁷ As shown in Figure 2, four characteristic bands appeared in the IR spectra of the $\text{H}_4\text{SiMo}_{12}\text{O}_{40}$ /PVA fiber mats. The intensity of the four characteristic bands increased with an increasing $\text{H}_4\text{SiMo}_{12}\text{O}_{40}$ content, indicating that the PVA had been doped with $\text{H}_4\text{SiMo}_{12}\text{O}_{40}$.

XRD spectra

Figure 3 gives the XRD pattern for different $\text{H}_4\text{SiMo}_{12}\text{O}_{40}$ /PVA fiber mats. For pure PVA fiber mats, as is known, there is a peak around $2\theta = 20^\circ$, which corresponds to the (101) plane of semicrystalline PVA.² Here, the crystallinity is high due to the hydroxyl groups in the side chain. However, as shown in Figure 3, the peak almost disappears with an increasing $\text{H}_4\text{SiMo}_{12}\text{O}_{40}$ content. These results illustrate that the crystal growth of PVA was extremely inhibited by the $\text{H}_4\text{SiMo}_{12}\text{O}_{40}$ and PVA became an amorphous state. The appearance of a special peak at $2\theta < 10^\circ$ was observed for the fiber mats containing $\text{H}_4\text{SiMo}_{12}\text{O}_{40}$. The peak appeared, shifted toward high 2θ , and became sharp with an increasing $\text{H}_4\text{SiMo}_{12}\text{O}_{40}$ content. As shown in Figure 3, there was no peak for the 20 wt % $\text{H}_4\text{SiMo}_{12}\text{O}_{40}$ fiber mats. One peak appeared at $2\theta = 5.7^\circ$ and $d = 15.48\text{ \AA}$ for the 50 wt % $\text{H}_4\text{SiMo}_{12}\text{O}_{40}$ fiber mats and one peak appeared at $2\theta = 7.6^\circ$ and $d = 11.62\text{ \AA}$ for the 80 wt % $\text{H}_4\text{SiMo}_{12}\text{O}_{40}$ fiber mats. Polymer doped with simple inorganic acids led to a more ordered structure with relatively distinct Bragg reflections.¹⁸ Obviously, the appearance of the peak at $2\theta < 10^\circ$ indicates that the molecules of the fiber mats are in order, with a short interlayer

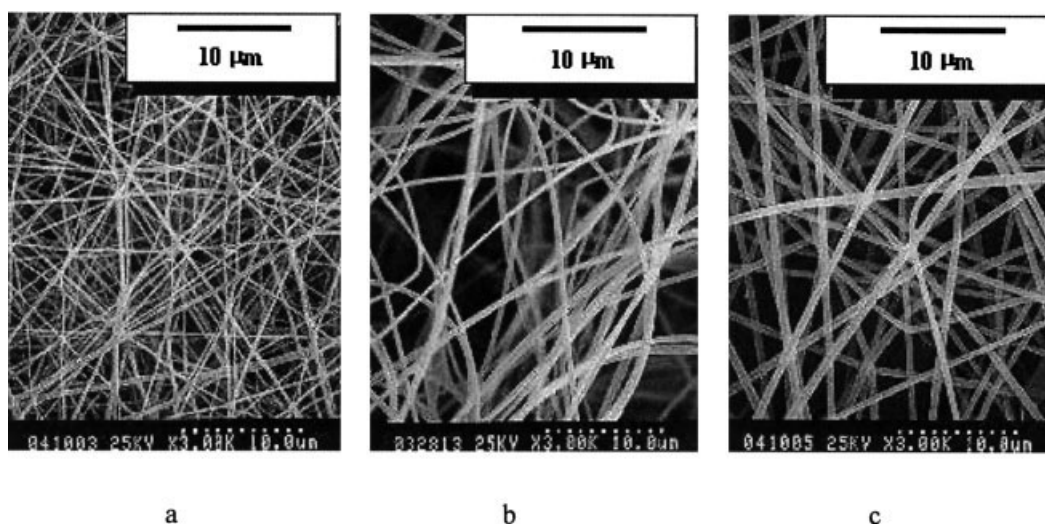


Figure 5 SEM of various $\text{H}_4\text{SiMo}_{12}\text{O}_{40}$ /PVA fiber mats with different $\text{H}_4\text{SiMo}_{12}\text{O}_{40}$ content: (a) 20 wt %; (b) 50 wt %; (c) 80 wt %.

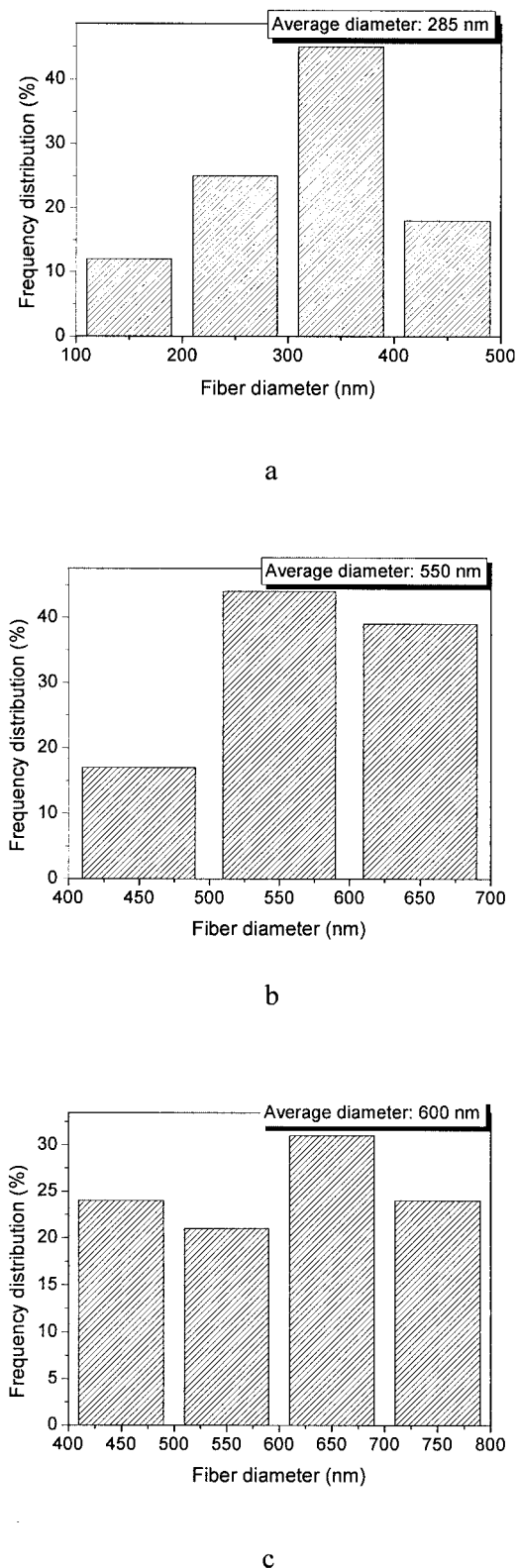


Figure 6 Frequency distribution of H₄SiMo₁₂O₄₀/PVA fiber mats with different H₄SiMo₁₂O₄₀ content: (a) 20 wt %; (b) 50 wt %; (c) 80 wt %.

distance.¹⁹ The shift of the peak from $2\theta = 5.7^\circ$ $d = 15.48 \text{ \AA}$ to $2\theta = 7.6^\circ$ $d = 11.62 \text{ \AA}$ indicates that the repeat distance of the polymer decreases with an increasing H₄SiMo₁₂O₄₀ content. The peak was moved closer to the characteristic peak of polyoxometalate with an increasing H₄SiMo₁₂O₄₀ content.²⁰ No peaks from any crystalline form of H₄SiMo₁₂O₄₀ could be observed, indicating that H₄SiMo₁₂O₄₀ was inserted into the PVA matrix.²¹

DSC

The DSC thermograms of the H₄SiMo₁₂O₄₀/PVA fiber mats are shown in Figure 4. The endothermic curve of pure PVA showed a peak at about 200°C. The melting temperature of the H₄SiMo₁₂O₄₀/PVA fiber mats shifted toward the low temperature with an increasing H₄SiMo₁₂O₄₀ content. The last melting temperature was about 155°C when the H₄SiMo₁₂O₄₀ content was 80 wt %. This indicated that the ordered association of the PVA molecules was decreased by the presence of H₄SiMo₁₂O₄₀.²² A special situation was obtained as shown in Figure 4: The endothermic peak became a broader peak for the 20 wt % H₄SiMo₁₂O₄₀/PVA fiber mats. The broadening of the endothermic peak supports the above-mentioned view. However, the endothermic peak became sharper with an increasing H₄SiMo₁₂O₄₀ content. This suggested that the molecule layer order of the fiber mats increased with a further increase in the H₄SiMo₁₂O₄₀ content.

SEM

Figure 5 gives SEM photographs of various fiber mats. Fiber mats with different H₄SiMo₁₂O₄₀ content had a regular morphology with variations in the diameter. The diameter distributions as a function of concentration are shown in Figure 6. As observed in Figures 5 and 6, the diameter of the fibers increases as the concentration increases. The average diameter of the fibers changed from 285 to 600 nm with an increase in H₄SiMo₁₂O₄₀ content from 20 to 80 wt %. Another interesting observation was that the fiber junctions decreased with an increasing H₄SiMo₁₂O₄₀ content in the PVA solution. We deduced that these apparent junctions were formed by an overlap of the fibers because of the viscosity behavior of the PVA solution. These results indicate that the addition of H₄SiMo₁₂O₄₀ to the PVA solution might produce a homogeneous species formed by interaction between the PVA and H₄SiMo₁₂O₄₀ molecules. Thus, fiber mats with regular morphologies can be prepared. As a result, higher H₄SiMo₁₂O₄₀ contents produce wider diameter fibers and fewer fiber junctions, influencing the morphologies.

Effect of viscosity and conductivity of the solutions on diameter of the fibers

Table I shows the viscosity and conductivity of different $H_4SiMo_{12}O_{40}$ /PVA solutions and the diameter of the fibers. The viscosity decreased and the conductivity increased with an increasing $H_4SiMo_{12}O_{40}$ content. At the same time, the diameter of the fibers increased with an increasing $H_4SiMo_{12}O_{40}$ content. Usually, the fiber diameter was affected by the viscosity and conductivity of the solution. As the viscosity of the solution was increased, the fiber diameter became larger; as the net charge density was increased, the fiber diameter became smaller.²³ However, the present results are inverse here. The experiment showed that the diameter of the fibers increased with a decreasing viscosity of the solutions and increasing conductivity of the solutions. We deduce that the inverse result comes from the higher $H_4SiMo_{12}O_{40}$ content and higher ion charge. This does, however, need to be further investigated.

Swelling in water

The ability to imbibe large quantities of water has made PVA useful for many superabsorbent applications.²⁴ Figure 7 shows the swelling curve of water uptake of $H_4SiMo_{12}O_{40}$ /PVA fiber mats. The $H_4SiMo_{12}O_{40}$ /PVA fiber mats were treated at 70 and at 125°C for 12 h. The results of the experiment showed that the degree of swelling decreased with an increasing $H_4SiMo_{12}O_{40}$ content and heat-treatment temperature. As we know, PVA was soluble in water. It became insoluble in water for a sufficiently large degree of crosslinking. Usually, the degree of crosslinking was affected by the heat treatment. In a range of treatment temperature, the degree of crosslinking increased with an increasing treatment temperature.²⁵ Figure 7 shows that the water content in the fiber mats decreased with an increasing temperature for the fiber mats treated. Here, the water uptake of pure PVA fiber mats treated at 125°C for 12 h was also checked. The water uptake of the pure PVA fiber mats was 20.2 g/g. At the same condition, the water uptake of the fiber mats with a 20 wt % $H_4SiMo_{12}O_{40}$ content was 2.8 g/g. The PVA content changed only

TABLE I
Data of Viscosity and Conductivity of the Solutions and Diameter of the Fibers

Content of $H_4SiMo_{12}O_{40}$	Viscosity (cp)	Conductivity (s/m)	Diameter of fibers (nm)
20 wt %	512.7	1.04	285
50 wt %	140.0	3.78	550
80 wt %	110.4	11.51	600

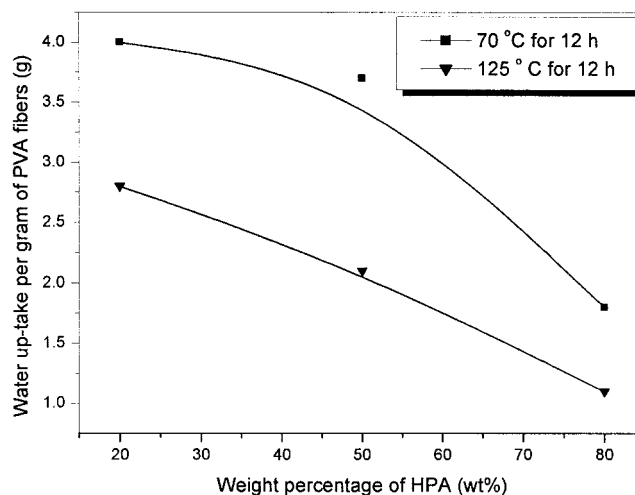


Figure 7 Water uptake per gram of the PVA fiber mats with different heat-treatment temperatures and $H_4SiMo_{12}O_{40}$ content.

from 100 to 80 wt %; however, the change of the water uptake attained was 17.4. Obviously, $H_4SiMo_{12}O_{40}$ resulted in the crosslinking of the PVA. All this indicates that the higher the $H_4SiMo_{12}O_{40}$ content and the heat-treatment temperature the higher is the crosslinking density of the PVA fibers and the less is the swelling in water. These results show that PVA having a higher $H_4SiMo_{12}O_{40}$ content and treated at higher temperature was more stable and swelled less.

CONCLUSIONS

For the first time, fiber mats of $H_4SiMo_{12}O_{40}$ /PVA were successfully prepared by the electrospinning technique. XRD and DSC indicated that PVA fiber became amorphous with an increasing $H_4SiMo_{12}O_{40}$ content. However, the molecules of the fibers were in order with a short interlayer distance with an increasing $H_4SiMo_{12}O_{40}$ content. SEM showed that the average diameter of the fibers was about 285–600 nm. The diameter of the fiber mats increased with an increasing $H_4SiMo_{12}O_{40}$ content and conductivity of the solution and decreasing viscosity of the solution. The degree of swelling decreased with an increasing $H_4SiMo_{12}O_{40}$ content and heat-treatment temperature.

This work was supported by a grant of the Post-Doctoral Program, Chonbuk National University (2001–2002), South Korea.

References

- Mayer, C. R.; Cabuil, V.; Lalot, T.; Thouvenot, R. *Angew Chem Int Ed* 1999, 38, 3672.
- Nakane, K.; Yamashita, T.; Iwakura, K.; Suzuki, F. *J Appl Polym Sci* 1999, 74, 133.

3. Formhals, A. U.S. Patent 1 975 504, 1934.
4. Bognitzki, M.; Czado, W.; Frese, T.; Wendorff, J. H. *Adv Mater* 2001, 13, 70.
5. Huang, L.; McMillan, R. A.; Apkarian, R. P.; Pourdeyhimi, B.; Chaikof, E. L. *Macromolecules* 2000, 33, 2989.
6. Bognitzki, M.; Hou, H.; Ishaque, M.; Frese, T.; Hellwig, M.; Schwarte, C.; Schaper, A.; Wendorff, J. H.; Grwiner, A. *Adv Mater* 2000, 12, 637.
7. Bergshoef, M. M.; Vancso, G. J. *Adv Mater* 1999, 11, 1362.
8. Doshi, J.; Reneker, D. H. *J Electrostat* 1995, 35, 151.
9. Norris, I. D.; Shaker, M. M.; Ko, F. K.; MacDiarmid, A. G. *Synth Met* 2000, 114, 109.
10. Pope, M. T.; Muller, A. *Polyoxometalates: From Platonic Solids to Anti-retroviral Activity*; Kluwer: Dordrecht, The Netherlands, 1994; pp 18–47.
11. Berzelius, J.; Poggendorffs *Ann Phys* 1826, 6, 369.
12. Zhang, T. R.; Feng, W.; Lu, R.; Zhang, X. T.; Jin, M.; Li, T. J.; Zhao, Y. Y.; Yao, J. N. *Thin Solid Films* 2002, 402, 237.
13. Stangar, U. L.; Grosej, N.; Orel, B.; Schmitz, A.; Colomban, P. *Solid State Ion* 2001, 145, 109.
14. Muller, A.; Kogerler, P.; Kuhlmann, C. *J Chem Soc Chem Commun* 1999, 1347.
15. Wu, Q. Y.; Wang, H. B.; Yin, C. S.; Meng, G. Y. *Mater Lett* 2001, 50, 61.
16. Qu, L. Y.; Shan, Q. J.; Gong, J. *J Chem Soc Dalton Trans* 1997, 4525.
17. *Encyclopedia of Polymer Science Engineering*; Marten, F. L.; Kroschwitz, J. I., Eds.; Wiley: New York, 1989; Vol. 17, pp 169, 179.
18. Pouget, J. P.; Jozefowicz, M. E.; Epstein, A. J.; Tang, X.; MacDiarmid, A. G. *Macromolecules* 1991, 24, 779.
19. Gong, J.; Cui, X. J.; Xie, Z. W.; Wang, S. G.; Qu, L. Y. *Synth Met*, in press.
20. Wu, Q.; Tao, S.; Lin, H.; Meng, G. *Mater Sci Eng B* 2000, 68, 161.
21. Qu, L. Y.; Lu, Q. R.; Peng, J.; Chen, Y. G.; Dai, Z. M. *Synth Met* 1997, 84, 135.
22. Krumova, M.; Lopez, D.; Benavente, R.; Mijangos, C.; Perena, J. M. *Polymer* 2000, 41, 9265.
23. Fong, H.; Chun, I.; Reneker, D. H. *Polymer* 1999, 40, 4585.
24. Martens, P.; Anseth, K. S. *Polymer* 2000, 41, 7715.
25. Ding, B.; Kim, H. K.; Lee, S. C.; Shao, C. L.; Lee, D. R.; Park, S. J.; Kwag, G. B.; Chol, K. J. *J Polym Sci Part B Polym Phys* 2002, 40, 1261.